T.3: Studies on Thin Films and Quantum Structures of ZnO Grown by Pulsed Laser Deposition

Pankaj Misra (pmisra@rrcat.gov.in)

1. Introduction and Overview

Zinc Oxide (ZnO) has stayed at the focal point of research and development on materials for more than last six decades due to unusual blend of its physical and chemical properties [1, 2]. ZnO is a wide bandgap II-VI oxide semiconductor with a direct bandgap of ~ 3.3 eV at room temperature and thus highly transparent in visible spectral region with sharp cut off at ~ 375 nm. It is naturally accruing n-type semiconductor and one of the most radiation hard materials. It is non toxic and environmental friendly. ZnO is inherently pyroelectric, piezoelectric, piezo-optic, luminescent and good thermal conductor etc. Alloying and doping ZnO with other common oxides make it possible to tailor its properties in a broad range for device applications.

ZnO has long history of use in different forms in various industrial and scientific applications. It has found applications as transparent conducting electrodes for solar cells, high frequency surface acoustic wave (SAW) devices, piezoelectric transducers, varistors, green phosphor for display devices and sensors etc. Of late quantum structures of ZnO such as quantum wells, wires and dots etc. have attracted much attention primarily to investigate their novel characteristics arising due to size effects. The genesis of current surge of interest in ZnO is essentially to develop short wavelength photonic and transparent electronic devices such as light emitting diodes, laser diodes, polariton lasers, solar blind UV photo-detectors, white light sources, resonant tunneling diodes, field effect transistors, field emitters and spin-photonic devices which are based on epitaxial thin films and quantum structures of ZnO of different dimensionality.

2. Pulsed Laser Deposition of ZnO

Pulsed Laser Deposition (PLD) is one of the popular growth methodologies to deposit thin films and quantum structures of ZnO under optimized conditions [1]. The technique uses high power laser pulses to ablate materials from their high density targets. This ablation event produces a transient, highly luminous plasma plume that expands rapidly away from the target surface. The ablated material is condensed on a solid substrate resulting in the formation of quantum structures or thin films depending upon the time and other deposition conditions. The growth process may be supplemented by a passive or a reactive ambient and under optimal conditions of deposition, the chemical composition of the target and the grown film remains same. Despite its inherent problems of particulates and large area scaling, PLD has emerged as a popular choice for the growth of complex oxide materials mainly due to its extreme simplicity, congruent evaporation and ease in handling reactive oxygen.

We have developed pulsed laser deposition set-up to grow ZnO thin films and quantum structure. Fig.T.3.1 shows the schematic of a PLD set-up which essentially contains a laser and vacuum chamber. The vacuum chamber is made of stainless steel and has a number of standard ports required for pumping, pressure and temperature gauges, gas inlet and laser inlet port etc. A turbo molecular pump was used to evacuate the deposition chamber. The substrate is loaded on to an appropriate electrical heater to provide high substrate temperature up to ~ 800 °C during the growth. The deposition chamber is equipped with a multi-target carrousel to accommodate maximum of six targets simultaneously to facilitate multilayer deposition. The target is continuously rotated and rastered during the ablation process to ensure uniform ablation of material from target surface. A pulsed laser system (third harmonic of a Q-switched Nd: YAG laser) was used to ablate the target material, which is placed at a certain distance in front of the substrate. The isolation of heating source i.e., laser from the growth chamber produces enormous facility in the growth of complex multilayer thin films and quantum structures and minimizes the thermal load on the growth chamber. The reactive gases such as O_2 can be introduced in to the vacuum chamber in controlled manner during the growth to perform reactive deposition.

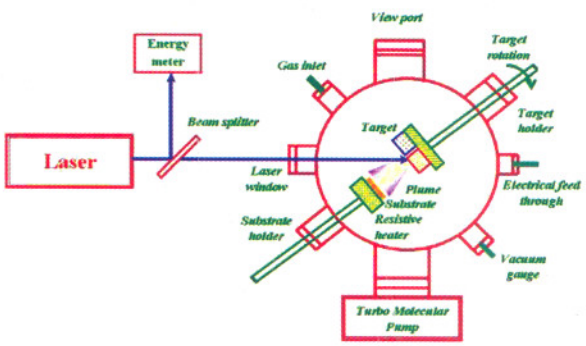

Fig.T.3.1 Schematic of the pulsed laser deposition setup

3. Results and Findings

We have carried out growth of high quality ZnO thin films, meta-stable ternary alloys and quantum structures such as multiple quantum wells and multilayer matrices of ZnO quantum dots of different sizes using optimized PLD methodology and studied their physical and chemical characteristics using verity of characterization techniques such as high resolution X-ray diffraction, optical absorption and transmission, Photoluminescence spectroscopy, Hall measurements, Secondary ion mass spectrometry, Rutherford back scattering spectroscopy, scanning and tunneling electron microscopy etc. The results of these studies and important findings will be discussed in detail in subsequent sections.

3.1 Time of Flight Mass Spectrometry of ZnO Ablation Plume

In case of PLD the physical and chemical composition of the deposited structures depends upon the composition of laser ablated plume. We have studied the composition of laser ablated ZnO plasma plume using Time of Flight Mass Spectroscopy (TOF-MS) to know the ablation products and found that the ablation plume contains very complex species ranging from atoms to clusters with a distribution, which is highly dependent on the laser fluence used [3]. At low laser fluence of ~ 100 J/m^2 the ZnO plume mainly contains atomic and diatomic Zn and molecular ZnO and Zn_2O. Cluster formation was not visible in the mass spectrum at this fluence [3]. However the ZnO cluster formation was found to enhance significantly with increasing laser fluence and at high laser fluence of ~ 1250 J/m^2 the mass spectrum contain a complete series of $(ZnO)_n$ clusters up to sizes (n) ~ 20. For cluster sizes up to about 10, twin signals were identifiable, one peak corresponding to clusters of equal numbers of zinc and oxygen atoms, and an additional peak corresponding to clusters with an added zinc atom. The relative intensity of the latter species was found to drop with cluster size. In addition, clusters with two additional zinc atoms are formed up to n = 3. To avoid having stable clusters in the deposit, it is obvious that low laser fluence close to ablation threshold should be used.

3.2 Characteristics of PLD grown ZnO Films

We have studied the structural, optical and electrical characteristics of ZnO thin films grown using PLD under different conditions of depositions on (00.1) sapphire substrate to understand their basic nature. About 300 nm thick ZnO thin films were grown at different substrate temperatures in the range of 400- 750 °C. All the ZnO films deposited at different substrate temperatures showed only (0002) and (00.4) ZnO reflections in ω-2θ high resolution x-ray diffraction (HRXRD) patterns, indicating that the film growth took place along the c-axis. The FWHM of the ω-rocking curve of (00.2) ZnO peak for the ZnO thin films grown at 750 °C , which was ~ 0.11° increased up to 0.58° when grown at 400°C indicating deterioration in crystalline properties with decreasing temperature [4].

The in-plane orientations of ZnO lattice in the films grown at various temperatures in the range of 400-750°C on (00.1) sapphire was investigated using Φ-scans of HRXRD measurements and found to be growth temperature dependent. At low growth temperatures of 400°C the ZnO lattice was found to align with sapphire lattice with large in-plane lattice mismatch of ~31.8%. At higher growth temperatures (≥ 700°C) the ZnO lattice was found to be 30° rotated with respect to sapphire lattice. In this in-plane arrangement the lattice mismatch is ~18% which is further reduced to ~0.91% through domain epitaxy. As a result of the reduced strain the crystalline quality of ZnO on sapphire was found to improve with increasing temperature. The best crystalline quality of ZnO on Sapphire was found at the substrate temperature of 750°C with FWHM value of ω-scan of symmetric (00.2) and asymmetric (10.4) ZnO peak ~ 0.11° and 0.28° respectively.

However from the viewpoint of the device development, it is desired to grow high crystalline quality films at low temperatures. To accomplish this we have evolved a buffer assisted PLD scheme of ZnO [4]. This scheme envisages growing first a buffer layer of ZnO on sapphire at high temperature and subsequent ZnO thin films at low temperature. Consequently, it was found that high crystalline quality of the over layers with 30° in-plane rotated growth on sapphire can indeed be achieved even at low growth temperatures. The buffer assisted growth methodology also results in decreased surface roughness and provides the necessary condition for a sharp interface in a multilayer structure due to subdued elemental diffusion.

The effect of post deposition annealing on the structural properties of ZnO films was studied. ZnO thin films grown using PLD at 500°C were annealed at different temperatures in the range of 600-1000°C in air ambient. The mosaicity parameters such as tilt and twist of grains, lateral and vertical coherence length etc. have been extracted from the analysis of the line width of symmetric (00.2), (00.4), (00.6) and asymmetric (10.1) ZnO reflections using Williamson–Hall plots. The crystallographic tilt and twist between grains in ZnO layer and microstrain was found to decrease significantly on annealing up to 800°C and then increase marginally on further increase in the annealing temperature up to 1000°C. The lateral coherence length ie the grain size which was ~ 50 nm for as grown films increased up to ~700 nm on annealing at 800°C and remained nearly constant with further annealing up to 1000°C. The lateral grain size measured using SEM and AFM was found in close agreement to those extracted from HRXRD.

The as grown ZnO film was degenerate with high carrier concentration (~8×10^{18} cm^{-3}) and low electron mobility (~22 cm^2/V-s) primarily due to presence of point defects such as oxygen vacancies and Zinc interstitial etc., dislocations and grain boundaries. The carrier concentration was found to reduce up to ~ 7×10^{16} cm^{-3} and their mobility increased up to ~81 cm^2/V-s on annealing at 800°C. This reduction in carrier concentration and enhancement in their mobility on annealing at 800°C was attributed to the replenishment of oxygen vacancies which is one of the potential donor defects in ZnO, increase in grain size and annulment of structural defects respectively. However on annealing beyond 800°C, the electrical characteristics deteriorated marginally perhaps due to slight but monotonic increase in the dislocations and point defect density (microstarin) and deterioration in the chemical quality of the films due to the diffusion of Al into ZnO at the interface. From these observations a correlation between the

annealing temperatures and structural and electrical characteristics of ZnO thin films was established to elucidate the optimal annealing conditions.

Photoluminescence processes in the PLD grown ZnO thin film was studied in the broad temperature range of 10 to 300K to understand various recombination mechanisms and their relative influence on light emission process [5]. Fig.T.3.2 shows PL spectra of the ZnO thin film recorded at 10 different temperatures in the range of 10 to 300 K. To determine the individual peak position and its intensity within a spectrum, we reconstructed the spectrum using multiple standard Gaussian equations as shown in the inset. It was observed that the low temperature PL spectra were dominated by recombination of donor bound excitons (B_X) and their phonon replicas. With increasing temperature, free exciton (F_X) PL and the associated LO phonon replicas increased in intensity at the expense of their bound counterparts. The B_X peak with line width of ~6 meV at 10K exhibited thermal activation energy of ~ 17 meV, consistent with the exciton-defect binding energy. Variation of the spectral position of all the peaks as a function of temperature is shown in Fig.T.3.3. The separation between the F_X and B_X peak positions was found to reduce with increasing temperature, which was attributed to the transformation of B_X into the shallower donor bound exciton complexes at consecutive lower energy states with increasing temperature [5]. The energy separation between F_X peak and its corresponding 1-LO phonon replica showed stronger dependence on temperature than that of 2-LO phonon replica. However their bound counterparts did not exhibit this behavior. The observed temperature dependence of the energy separation between the free exciton and it's LO phonon replicas are explained by considering the kinetic energy of free exciton. The observed PL transitions and their dynamics at different temperatures are consistent with observations made with bulk ZnO crystals implying high crystalline and optical quality of the grown films [5].

3.3 Bandgap engineering of ZnO

Bandgap engineering of ZnO, which is essential to realize its quantum structures, was carried out by alloying it with other binary oxides such as MgO and CdO etc [6-8]. Although the thermodynamic solid solubility limit of MgO and CdO in ZnO is limited to only ~4% and 2% respectively, the PLD, due to its non equilibrium growth nature could enable the metastable alloying of $Mg_xZn_{1-x}O$ and $Cd_xZn_{1-x}O$ with Mg and Cd concentration much beyond the solubility limits. The bandgap of $Mg_xZn_{1-x}O$ films was found to increase monotonically from ~3.3 to 4.2 eV, as shown in Fig.T.3.4 with increasing Mg concentration up to ~ 39% in the films beyond which segregation of cubic phase MgO in wurtzite phase $Mg_xZn_{1-x}O$ was observed using HRXRD and shown in inset of same figure. Up to ~ 39% concentration of Mg, the alloy films were found to be strained but mostly single phase and c-axis oriented.

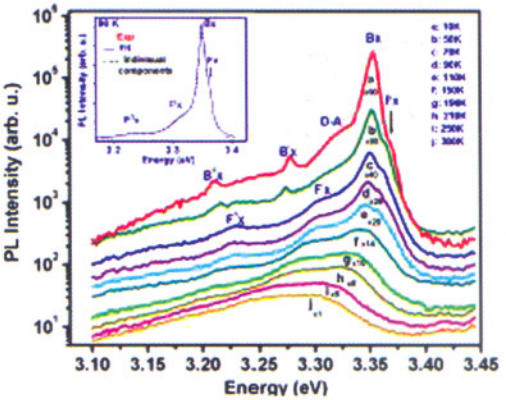

Fig.T.3.2 Photoluminescence spectra of ZnO thin film at different temperatures in logarithm scale Inset shows the fitting procedure (solid) for 90K PL spectrum using Gaussian components (dotted)

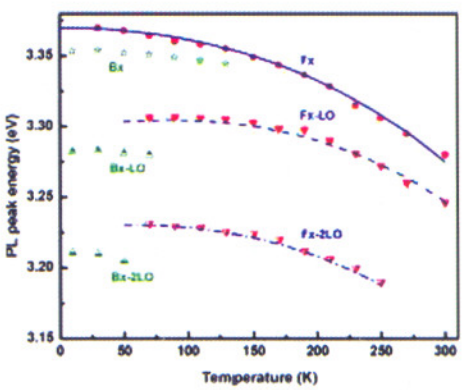

Fig.T.3.3 Temperature dependence of energy positions of free and bound exciton PL and associated phonon replicas. Solid line shows the theoretical fits

We have evolved variable oxygen ambient pressure based PLD methodology to continuously vary the ZnO bandgap using single MgZnO target with fixed concentration of Mg [6]. It was observed that the bandgap of $Mg_xZn_{1-x}O$ thin films grown using a sintered pallet of MgZnO containing 10 mole % of MgO mixed in ZnO can indeed be controlled in the range of ~3.45 to 3.8 eV only by changing the oxygen partial pressure from 10^{-2} to 10^{-5} Torr during the growth. The change in the bandgap of $Mg_xZn_{1-x}O$ films grown at different oxygen partial pressures was attributed to change in the Mg concentration in the resulting films.

Alloy thin films of $Cd_xZn_{1-x}O$ with different Cd concentrations were grown by sequential ablation of ZnO and CdO targets alternately to decrease the bandgap of the intrinsic ZnO [8]. The Cd concentration in the films, measured by Rutherford back scattering, was varied by controlling the ablation time of the CdO target relative to that of the ZnO. The films were found to be of a c-axis-oriented wurtzite phase with high crystalline quality up to a Cd concentration of ~ 8%,

beyond which CdO segregation occurred. Fig.T.3.5 shows the optical transmission spectra of $Cd_xZn_{1-x}O$ thin films with different Cd concentrations. The band gap of the $Cd_xZn_{1-x}O$ thin films was found to decrease monotonically from ~ 3.3 to 2.9 eV with increasing x until the onset of CdO segregation. However, in cases of both these ternary alloys the collective effect of crystal defects and strain, as reflected by the HRXRD patterns, was within the limits required for the growth of ZnO-based quantum well structures [8].

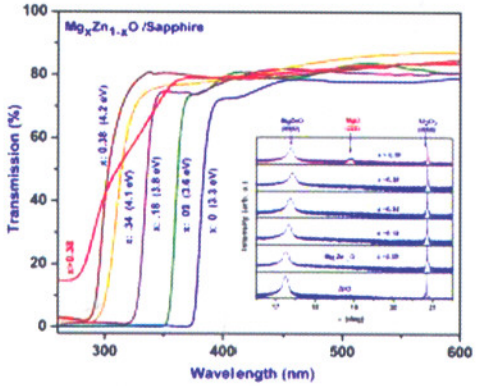

Fig.T.3.4 Transmittance spectra of $Mg_xZn_{1-x}O$ thin films with different Mg concentrations. Inset shows bandgap of $Mg_xZn_{1-x}O$ as a function of Mg concentration

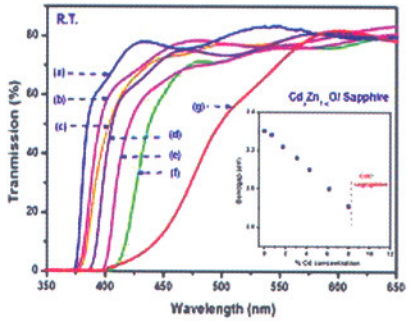

Fig T.3.5 transmission spectra of ZnO (a) and $Cd_xZn_{1-x}O$ thin films with (b) x~0.018 (c) x~0.031 (d) x~0.06 (e) x ~ 0.08 and (e) x > 0.08. Inset shows the band gap of $Cd_xZn_{1-x}O$ thin films with varying Cd concentrations

3.4 Studies on ZnO Multiple Quantum Wells

We have grown ZnO/ $Mg_{0.36}Zn_{0.64}O$ multiple quantum wells (MQW) of well layer thickness in the range of ~1 to 4 nm on Sapphire substrates by PLD using an in–house developed buffer assisted growth scheme under highly optimized conditions [2,9,10]. The schematic of ZnO/MgZnO MQWs is shown in inset of Fig.T.3.6. The thickness of $Mg_{0.36}Zn_{0.64}O$ barrier layer was kept constant at 8 nm. With these MQWs we have succeeded in observing an efficient room temperature PL, which to the best of our knowledge has been achieved for the first time. We have studied the photoabsorption and PL spectra of these MQWs and established a relationship between their band-gap and the thickness of the corresponding well layers.

Fig.T.3.6 shows the room temperature optical absorption spectra of ZnO MQW structures which clearly showed the monotonic blue shift in ZnO absorption edge due to quantum confinement effect and excitonic features entwined with the band edges [8, 9]. At room temperature the band edge of these MQWs shifted from ~3.36 to 3.78 eV on decreasing the well layer thickness from ~4 to 1 nm in agreement with theoretically calculated values.

The Photoluminescence spectra of ZnO MQWs of different well layer thicknesses and at different temperatures in the range of 10- 300K is shown in Fig.T.3.7. It can be seen that the PL peak shifts towards blue with decreasing well layer thickness due to quantum confinement effects. Temperature dependence of the PL peak for the ZnO MQWs with well layer thickness of ~2.5 nm is also shown in Fig.T.3.7 [2, 9, 10]. The bandgaps of ZnO MQWs with different thicknesses obtained from PL and absorption spectra and from theoretical calculations are shown in inset of Fig T.3.7

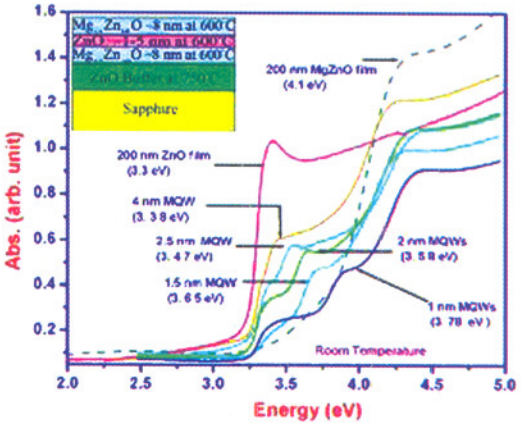

Fig.T.3.6 Optical absorption spectra of ZnO MQWs and 200 nm thick films of ZnO and $Mg_{0.34}Zn_{0.66}O$ at RT. The values in the parentheses show the respective band gaps in eV. The inset shows the schematic of the ZnO/ $Mg_xZn_{1-x}O$ MQW

Temperature dependence of the PL line width (FWHM) for the ZnO MQWs with well layer thickness of ~2.5 nm is shown in Fig. T.3.8. It can be seen that the FWHM of the PL peak increases gradually up to ~ 120K and then exponentially up to RT. The temperature dependence of this line width was explained by considering the scattering of excitons with acoustic and optical phonons in different temperature regimes [9, 10]. In the range from 10 K to RT, the PL peak shifted monotonically towards red with increasing temperature as shown in Fig T.3.8. The red shift of the PL peak with

increasing temperature was attributed to the band gap shrinkage in accordance with the Varshni's relation.

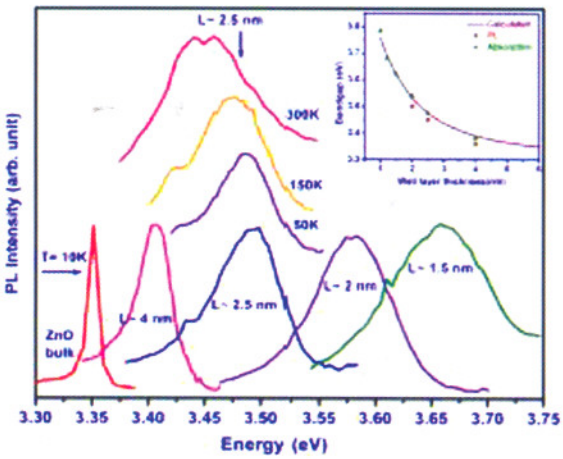

Fig.T.3.7 10K Photoluminescence from 200 nm thick ZnO film, ZnO MQWs with different active layer thicknesses. Vertical column shows the PL spectra of ZnO MQWs at a constant well layer thickness ~ 2.5 nm at four different temperatures down to room temperature. Inset in figure shows bandgap obtained from absorption and PL spectra as a function of well layer thickness at RT. Solid curve shows theoretically calculated values.

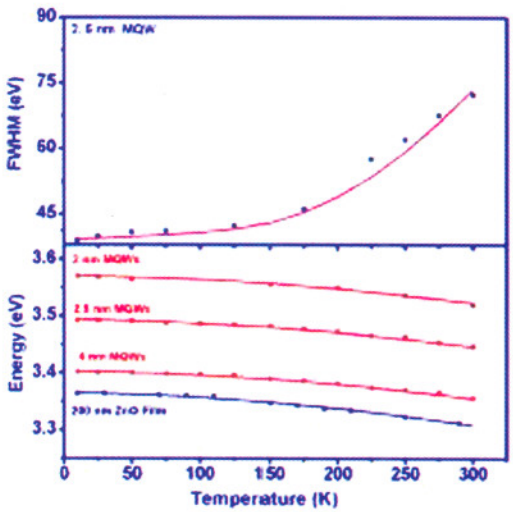

Fig.T.3.8 Variation of PL spectral line width with temperature from ZnO MQWs of well layer thickness of ~ 2.5 nm. Solid line shows the fitted theoretical dependence. (b) Temperature dependence of the PL peak position of ZnO MQWs with different well layer thicknesses and 200 nm thick ZnO film. Solid lines show the theoretical using the Varshani's relation.

3.4 Studies on ZnO Quantum Dots

We have also grown multilayer of Alumina capped ZnO quantum dots of different mean in-plane radii in the range of ~1.8 – 3.6 nm on Sapphire substrates using alternate PLD [2, 11]. The size of ZnO QDs was controlled by the ablation time of ZnO target. The mean in-plane radius, size distribution and density of the QDs were measured using Transmission Electron Microscope (TEM). The typical TEM micrograph for the QDs of mean in-plane radius of ~ 2.5 nm and their collective selected area diffraction pattern is shown in Fig.T.3.9. The size variation about the mean size was ~30% with density in the range of 10^{10}–10^{11}/cm^2 [11]. It was also observed that size distribution is not symmetric around the mean diameter. The atomic force micrograph of typical ZnO QDs as shown in inset of Fig.T.3.9 revealed pyramidal shape of these dots. The absorbance spectra of alumina capped ZnO QDs grown for different times are shown in Fig.T.3.10. These absorbance spectra do not show a series of isolated absorption peaks, which is expected due to the broad distribution of QD sizes. Each spectrum, corresponding to a particular growth time and hence a mean size exhibits rather a broad absorption feature which is found to be due to the $1s_e - 1s_h$ transition [2, 11]. In Fig.T.3.10, one can clearly see that as the deposition time decreased the optical band-edge of the QDs blue-shifted as compared to the bulk band gap that corresponds to 375 nm. The observed blue shift in the ZnO band edge can be attributed to size dependent quantum confinement effect.

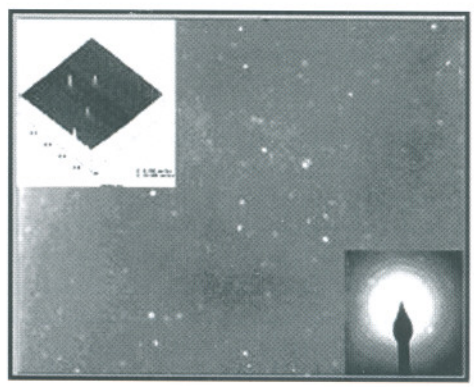

Fig.T.3.9 TEM micrographs of ZnO QDs deposited for 10 sec. A typical selective area electron diffraction pattern of the ZnO QDs and atomic force micrograph are shown in top left and bottom right inset.

The band gap of the ZnO quantum dots, measured from the photo absorbance data at different deposition times, is plotted as a function of the corresponding mean particle size measured from TEM in inset of Fig.T.3.10. The band gaps of the ZnO nano-particle matrices sifted towards blue with decreasing nanoparticles' size. In this figure one can clearly see a drastic increase in the band gap with decreasing size of the ZnO QDs in the range smaller than the excitonic Bohr

radius (a_B) for ZnO which is calculated to be ~ 2.1 nm. In the size range greater than the excitonic Bohr radius, the variation of the band gap is rather subdued as can be seen in this figure. The widest bandgap of ~ 4.5 eV was obtained for the particles of the smallest mean radius, i.e. 1.8 nm [7, 11].

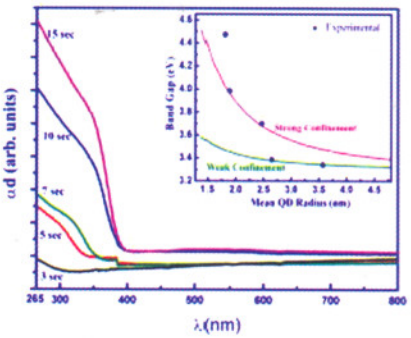

Fig.T.3.10 Absorbance spectra of alumina capped ZnO QDs grown for different times. Inset shows the variation of ZnO bandgap with quantum dot radius. Experimental data are shown by full circles Solid lines show theoretically calculated values

To understand these observations in two size-domains i.e. the dot size shorter than the excitonic Bohr radius and other one with the dot size larger than the excitonic Bohr radius; we have used the effective mass approximation with strong confinement and weak confinement respectively [7, 11]. The observed blue shift could be understood using the effective mass approximation in weak and strong confinement regimes.

4. Conclusions

In conclusions we have developed pulsed laser deposition facility to grow high quality ZnO thin films and quantum structures of different dimensionality. We have optimized deposition conditions for the growth of ZnO layers, ternary alloys and nanostructures with superior structural, optical and electrical characteristics. Controlled growth of ZnO quantum structures such as multiple quantum wells and quantum dots have been accomplished wherein size dependent blue shift in ZnO bandgap was observed due putative quantum confinement effects in line with theoretical models.

5. Acknowledgements

The author would like to express his sincere gratitude and thanks to his thesis advisor Prof. L. M. Kukreja for his kind guidance and care during the entire course of the thesis work. Timely support and co-operation of friends and colleagues from RRCAT and collaborators from Indian Institute of Technology Kanpur, Tata Institute of Fundamental Research, Mumbai, Indira Gandhi Center for Atomic Research, Kalpakam, UGC-DAE Centre for Scientific Research, Indore and Universities of Muenster and Ulm, Germany are highly acknowledged.

References:

[1]. L. M. Kukreja, B. N. Singh and P. Misra, Pulsed Laser Deposition of Nanostructured Semiconductors in Bottom-Up Nanofabrication: Supramolecules, Self-Assemblies and Organized Films, Eds. K. Ariga and H. S. Nalwa, American Scientific, California, chapter 9, pp. 235-274 (2009)

[2]. L. M. Kukreja, P. Misra, J. Fallert, J. Sartor, H. Kalt and C. Klingshirn; Nano-ZnO in Photonics Landscape; IEEE Proc. Photonic Global, ISBN: 978-1-4244-3901-0, 1-6 (2009)

[3]. L.M. Kukreja, A. Rohlfing, P. Misra, F. Hillenkamp and K. Dreisewerd, Cluster Formation in UV Laser Driven Ablation Plumes of ZnSe and ZnO Studied by Time-of-Flight Mass Spectrometry; Appl. Phys. A 78, 641– 644 (2004)

[4]. P. Misra and L. M. Kukreja, Buffer Assisted Low Temperature Growth of High Crystalline Quality ZnO Films using Pulsed Laser Deposition; Thin Solid Films 485 (1-2), 42-46 (2005)

[5]. P. Misra, T. K. Sharma and L. M. Kukreja, Temperature Dependent Photoluminescence Processes in ZnO Thin Films Grown on Sapphire by Pulsed Laser Deposition; Current Applied Physics 9, 179–183 (2009)

[6]. P. Misra, P. Bhattacharya, K. Mallik, S. Rajagopalan, L. M. Kukreja and K.C. Rustagi, Variation of Bandgap with O_2 Pressure in MgZnO Thin Films Grown by Pulsed Laser Deposition; Solid State Commun. 117, 673-677 (2001)

[7]. L. M. Kukreja, S. Barik and P. Misra, Variable Band-gap ZnO Nanostructures Grown by Pulsed Laser Deposition; Jr. Crystal Growth 268 (3-4), 531-535 (2004)

[8]. P. Misra, P. K. Sahoo, P. Tripathi, V. N. Kulkarni, R. V. Nandedkar and L. M. Kukreja, Sequential Pulsed Laser Deposition of $Cd_xZn_{1-x}O$ Alloy Thin Films for Engineering ZnO Band-gap; Appl. Phys. A 78, 37-40 (2004)

[9]. P. Misra, T. K. Sharma, S. Porwal and L. M. Kukreja, Room Temperature Photoluminescence from ZnO Quantum Wells Grown on (0001) Sapphire using Buffer Assisted Pulsed Laser Deposition; Appl. Phys. Lett. 89, 161912 (2006)

[10]. P. Misra, T. K. Sharma and L. M. Kukreja, Temperature Dependent Photoluminescence from ZnO/MgZnO Multiple Quantum Wells Grown by Pulsed Laser Deposition; Superlattices and Microstructures 42 (1-6), 212-217 (2007).

11. S. Barik, A. K. Srivastava, P. Misra, R. V. Nandedkar and L. M. Kukreja, Alumina Capped ZnO Quantum Dots Multilayer Grown by Pulsed Laser Deposition; Solid State Commun. 127, 463-467 (2003)